

In-Vivo Turbulent Stresses of Bileaflet Prosthesis Leakage Jets

Brandon R. Travis^{1,2}, Thomas D. Christensen^{1,2}, Morten Smerup^{1,2},
Morten S. Olsen^{1,2}, J. Michael Hasenkam^{1,2}, Hans Nygaard^{1,3}

¹Department of Cardiothoracic and Vascular Surgery and ²Institute for Experimental Clinical Research, Århus University Hospital, Skejby Sygehus, Århus, ³The Engineering College of Århus, Århus, Denmark

Background and aim of the study: Previous studies of leakage jet turbulence have been carried out in vitro, using a Newtonian fluid to simulate blood and large, rigid approximations to the chambers of the heart. The study aim was to apply an in-vivo method of quantifying leakage jet turbulence to a variety of bileaflet mechanical heart valves, and thereafter to determine the effects of exercise and valve design on turbulent shear stresses within leakage flow.

Methods: Bileaflet prostheses sewn to a manual traversing device were implanted in the mitral position of 29 pigs of body weight ca. 90 kg. Pulsed Doppler ultrasound was used to acquire velocity measurements within the leakage jets detected 1 mm upstream of the housing. Analytical techniques were used to estimate peak velocities and maximum turbulent shear stresses from these velocity measurements.

Results: Maximum turbulent shear stress was found to rise with increasing ventricular pressure. No leak-

age turbulence was found from a valve with relatively small leakage gap widths. The Medtronic Parallel® valve was found to have considerable significant leakage flow disturbance, even under low ventricular pressure conditions. Similar maximum turbulent shear stress magnitudes were estimated in the leakage jets of the St. Jude Medical®, CarboMedics® and Sorin Bicarbon® valves at medium ventricular pressure conditions. The maximum turbulent shear stresses estimated in these experiments were lower than those found in previous in-vitro measurements.

Conclusion: Exercise raises the turbulent shear stresses of leakage flow substantially. Hinge design and leakage gap width also affect the magnitudes of these stresses. Leakage flow turbulence may be less damaging to the blood than was previously thought, and is considerably less damaging than forward-flow turbulence.

The Journal of Heart Valve Disease 2005;14:644-656

Patients with mechanical heart valves have an increased risk of thromboembolic complications, and must undergo lifelong oral anticoagulation therapy. Although the specific characteristics of prostheses that promote such complications are currently unknown, theory, experimental evidence and clinical experience suggest that leakage flow is a potential culprit. Leakage flow is a distinct feature of mechanical prostheses; healthy natural valves and bioprostheses do not have gaps available for flow after closure, and consequently do not leak.

While forward-flow conditions are harshest across aortic valves, the harshest closure and leakage flow

conditions are found across mitral valves. Rates of thromboembolic complications are consistently higher for patients with mitral mechanical valve implants than those for patients with implants in any other position (1). During the period of the cardiac cycle when a mechanical valve is closed, transvalvular pressure gradients on the order of 100 mmHg drive blood through gaps only a few hundred microns in width. These conditions may create viscous stresses as high as 950 N/m² within the gaps (2). Perhaps more importantly, turbulent shear stresses within the leakage jets just beyond the gaps have been measured as high as 1,000 N/m² upstream of a tilting disc prosthesis (3). Erythrocytes are likely to rupture if exposed for a few milliseconds to turbulent shear stresses above 800 N/m² (4). As thrombocytes are more sensitive than erythrocytes to these mechanical stimuli (5), leakage flow through mechanical prostheses could be expected to rupture thrombocytes, releasing procoagulant pro-

Address for correspondence:
Brandon Travis, T-Forskning, Skejby Sygehus, Brendstrupgaardsvej,
8200 Århus N, Denmark
e-mail: brandontravis2001@yahoo.com

teins that initiate the coagulation cascade. Evidence of such stimulation has been observed in vitro (2,5). This theoretical and in-vitro experimental evidence is supported by clinical experience with the Medtronic Parallel® (MP) prosthesis. The MP design was withdrawn from the market in 1995 after poor performance in clinical trials; approximately 20% of patients in these trials developed thromboembolic complications (6). Explants from these patients showed that thrombus formation was localized to the pivot areas (7), the portion of the valve through which the vast majority of its leakage traverses.

Turbulent shear stresses due to the leakage flow of many prosthetic valve designs have been investigated in vitro (8-17). While impressive in what they have shown thus far, these simulations may not closely approximate the flow patterns and turbulence of mechanical prosthesis leakage flow. All of these studies have been performed in rigid simulators, using fluids that mimic the viscosity of blood at high shear rates. These simulators do not replicate the natural geometry of the circulation. In addition, the length scales of the leakage gaps are only one order of magnitude larger than the length scales of the blood cells themselves, which has been shown to cause blood to behave in a non-Newtonian fashion (18). As these possible shortcomings could have a large effect on the magnitudes of leakage jet turbulence, it may be necessary to study this turbulence in vivo, using whole blood and a physiologic cardiac geometry. In a previous technical report, a method was established for such a study (19). The aim of the present study was to apply this method to a variety of prosthetic valves, and thereafter to determine the effects of exercise and valve design on turbulent shear stresses measured in vivo in mechanical prosthesis leakage flow. The hypothesis was that turbulent shear stresses measured in vivo are less than those previously measured in vitro.

Materials and methods

Bileaflet valves were chosen for these studies because these valves are the most commonly used design. Bileaflet valves have a greater leakage volume than other mechanical valve designs, and have been shown to cause more hemolysis in patients than tilting-disc designs (20,21). The leakage flows of the MP, CarboMedics® Model 700 (CM), Sorin Bicarbon® (SB) and St. Jude Medical® Standard valve designs were investigated. Three St. Jude Medical Standard valves were studied. One of these was a clinical quality prosthesis (SJ), and the other two were provided by St. Jude Medical as being above and below their leakage tolerances; these are designated 'High Leaker' (HL) and 'Low Leaker' (LL) valves. Turbulent jets could not be

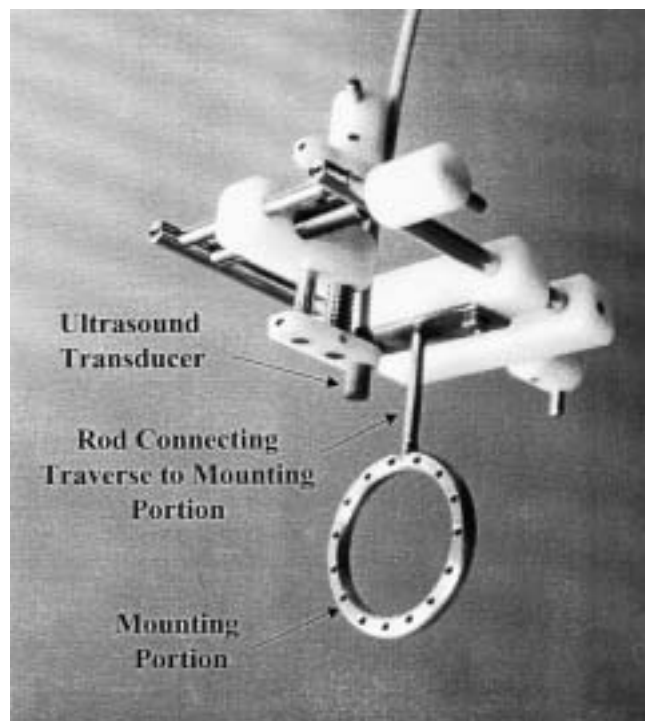


Figure 1: Traverse apparatus used to move ultrasound transducer. The mounting portion of the apparatus is sewn to the valve, allowing the precise positioning of an ultrasound transducer with respect to the valve. (Reproduced from Ref. (19), with permission from ASME publications.)

located in the LL valve, and therefore data from these experiments were not reported.

The methods used for these experiments are described in detailed fashion in a previous technical report (19). An abridged description of these methods is provided below.

Experimental set-up

Female pigs of body weight 90 kg were used as the experimental model. Twenty-nine pigs were used for these experiments, of which 12 were successful (two for each valve type). Unsuccessful experiments resulted either from refinement of the data collection technique ($n = 3$) or from death of the animal before the completion of data collection ($n = 14$).

On arrival at the laboratory, each pig was anesthetized, first intramuscularly and subsequently by access via an ear vein. Endotracheal intubation was carried out, and the pig was coupled to a ventilator. Anesthesia was maintained with midazolam (25 mg/kg/h), ketamine (1,250 mg/kg/h), and fentanyl (Haldid®; 1 mg/kg/h) throughout the experiment. An electrocardiogram and venous and arterial blood pressures were monitored continuously during the surgical

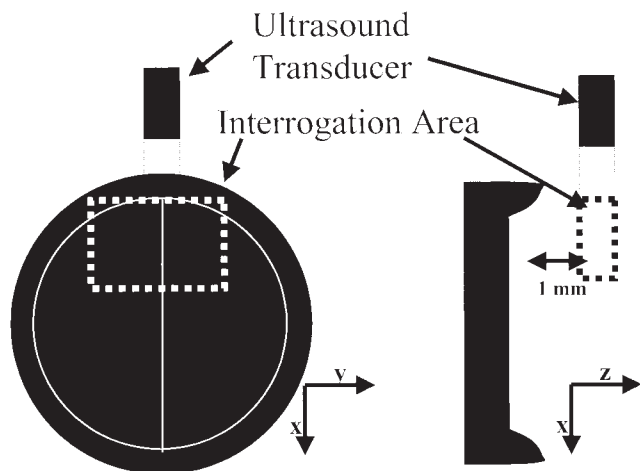


Figure 2: Interrogation area of study with respect to the valve and ultrasound transducer. The Cartesian axes used in this study are defined here. (Reproduced from Ref. (19), with permission from ASME publications.)

phase of the experiment.

A mid-line sternotomy was performed to expose the heart. After full heparinization, venous and aortic cannulae were introduced. Cardiopulmonary bypass (CPB) was then started to allow aortic cross-clamping and cold cardioplegic arrest. The mitral annulus was exposed using a left atrial incision. A size 29 mitral prosthesis was mounted and sewn tightly to a traverse apparatus (Fig. 1); this enabled an ultrasound transducer to be moved precisely in three dimensions with respect to the valve. The valve and mounting portion of the apparatus were implanted in the anti-anatomic position of the mitral annulus. The atrium was sutured around the traversing device in a way that allowed manual adjustment of transducer position during the experiment. The surgery simulated normal valve replacement, with the exception that the atrium was sewn around a small metal rod.

Pressure transducers (Model SPC-350; Millar Instruments, Inc., Houston, TX, USA) were inserted into both the left atrium and left ventricle. CPB was then terminated, and the heart was allowed to resume sinus rhythm. A custom-made 10-MHz ultrasound transducer was mounted on the traversing portion of the apparatus. This transducer was connected to a VingMed amplifier (Model ALFRED; VingMed, Horten, Norway), which was operated in the pulsed mode and modified to allow the measurement of turbulent velocity fluctuations. Previous tests on the pulsed Doppler ultrasound (PDU) system have quantified the -3 dB cut-off frequency of the ultrasound system at 200 Hz (22). The sample volume for this

apparatus was 1.5 mm in diameter and 1.0 mm in length. Amplifiers for the pressure and ultrasound transducers were interfaced with a computer.

Exercise conditions were simulated in half of the experiments by clamping the aorta until the peak left ventricular pressure rose to approximately 1.5-fold its resting value. Different pigs were used for the exercise and resting experiments, because the time needed to obtain measurements for both exercise and resting conditions was longer than most pigs could maintain a stable cardiac state. After the necessary measurements had been acquired, the pigs were euthanized by direct injection of a saturated potassium chloride solution into the left ventricle.

All procedures were conducted according to approval from the Danish Inspectorate of Animal Experimentation.

Data acquisition

An interrogation area 1 mm upstream of the valve housing (approximately 5 mm upstream of the pivots; Fig. 2) was defined using leakage jet angles determined from previous investigations (11). The traversing apparatus was adjusted until the ultrasound transducer contacted the atrial wall, and was moved through the interrogation area. Leakage jets were located by first listening to the Doppler sound. High frequencies were indicative of flow away from the transducer, and a sound with a broad range of frequencies was indicative of turbulence. Once a jet was located, a computer program that estimated turbulent stress magnitudes from mean velocity measurements of the ultrasound transducer was used to define a measurement area around the jet. These measurement areas were traversed in 0.5 mm spatial increments. When the ultrasound transducer was observed to be close to or within a jet, left atrial pressure, left ventricular pressure, and mean and maximum velocity signals from the VingMed amplifier were recorded at a rate of 5 kHz. Mean velocity signals were determined by averaging the range of Doppler shifts registered by the transducer after a single Doppler pulse. Maximum velocity signals were determined from the maximum in Doppler shift registered by the transducer after a single Doppler pulse. Therefore, the mean velocity signal represented the mean velocity of all blood cells within the sample volume at a particular time, while the maximum velocity signal represented the velocity of the single or small number of blood cells moving at the highest velocity within the sample volume at a particular time.

Data analysis

Data acquisition by the computer was triggered by a rise in ventricular pressure above 30 mmHg, and

Table I: Pig hemodynamic conditions during the study of the jets emitted from the pivots of each valve within the interrogation area.

Jet	Peak LVP (mmHg)*		Systolic duration (ms)+		Range
	Maximum	Minimum	Maximum	Minimum	
SJ R1	107	57	288	242	45
SJ R2	86	73	286	248	37
SJ E1	132	98	391	348	26
SJ E2	125	82	386	340	24
CM R1	121	91	398	304	54
CM R2	154	72	324	235	28
CM E1	198	161	378	272	42
CM E2	258	101	325	230	36
SB R1	115	56	249	149	26
SB R2	122	102	159	119	26
SB E1	124	109	362	315	26
SB E2	108	80	332	303	22
MP R1	96	79	350	252	59
MP R2	90	64	327	251	49
MP E1	247	184	309	203	84
MP E2	253	194	300	205	73
HL R1	98	64	297	198	73
HL R2	88	65	265	189	60
HL E1	130	114	445	352	69
HL E2	173	60	434	235	80

*Peak left ventricular pressure (LVP) represents the cyclic maximum in LVP.

+Systolic duration represents the period of the cardiac cycle during which the LVP was >30 mmHg.

Systolic duration range is the maximum range in systolic duration for cycles used in the analysis of a single measurement location.

Jets are designated first by valve design (SJ, CM, SB, MP, or HL). If an aortic clamp was used during the experiment, the jet was designated as being in an exercise (E) state. All remaining experiments were conducted in the resting (R) state. One pig study allowed the investigation of two jets (1, 2), one jet being emitted from each pivot immediately upstream of the interrogation area.

stopped when the pressure fell below 30 mmHg. The systolic duration was defined as the amount of time the ventricular pressure was greater than 30 mmHg within a given beat. Both systolic duration and peak left ventricular pressure varied within and between experiments. The minimum and maximum systolic duration and left ventricular pressure for each experiment are listed in Table I.

Acquired data were analyzed visually. If no velocity signal was present during a cycle, or if the left ventricular pressure signal during this cycle was markedly different from that of other cycles at the same measurement location, data from this cycle were removed from the analysis. Variation was inherent in the in-vivo models used, and when a cycle was markedly different from that of other cycles, usually larger differences could be seen in the left ventricular and atrial pressure curves than in the velocity traces for the same cycle. The exception to this was when the ultrasound transducer either did not have a solid contact with the tissue surface, or the sample volume contained the tissue

surface during portions of some of the cycles. Both velocity and pressure traces were examined for all cycles in order to remove errant cycles.

Due to differences in systolic duration within each experiment, placement of the remaining data with respect to time was normalized by systolic time duration. Mean and maximum velocity data in the remaining cycles were divided into 39 discrete phase windows for analysis. The time length of these windows depended on the systolic duration of a given beat, but the maximal length was 25 ms. This resulted in a minimum total of 1,175 measurements used to calculate mean velocity and turbulent normal stresses in each combination of measurement location and phase window.

Average velocities (u_{00}) within each of the phase windows were calculated by simple ensemble averaging of the maximum velocity measurements (u_{ij}):

$$(u_{00})_i = \frac{\sum_{j=1}^N \sum_{k=1}^N (u_{ij})_k}{N} \quad (1)$$

where a represents the number of cycles, n the number of measurements in the a^{th} cycle, and N the total number of measurements. These average velocity values represent only the velocity component in the direction of the ultrasound beam. To estimate peak velocity magnitudes in the jets (u_{peak}), these average velocities were corrected for direction:

$$u_{\text{peak}} = \frac{(u_{\text{av}})_x}{\cos\theta_x} \quad (2)$$

where θ_x is the angle between the x axis (defined in Fig. 2) and the axis of the leakage jet. Values of θ_x were estimated from previous studies (11,14), and are reported for each valve studied in Figure 3. It should be noted that the axes of the leakage jets did not lie on the same axis as the forward flow across the valve.

Turbulent normal stresses were calculated from both the mean and the maximum velocity measurements using a cyclic averaging technique (14):

$$\sigma_x = \frac{\sum_{i=1}^a \sum_{j=1}^n \rho (u_{ij}^2 - (u_{io})^2)}{N - a} \quad (3)$$

where u_{io} is the average velocity of the particular phase window in cycle i , u_{ij} is the single velocity measurement from cycle i (m/s), ρ is density (kg/m^3), and σ_x is the turbulent normal stress along direction of measurement (N/m^2).

These cyclic averaging calculations were corrected for errors resulting from Doppler ambiguity and velocity gradients across the sample volume. The calculated turbulent normal stresses were plotted in a temporal series of three-dimensional surface plots (an example of which is shown in Fig. 4) to ensure that the majority of the turbulent portion of the jet was captured by the acquisition process.

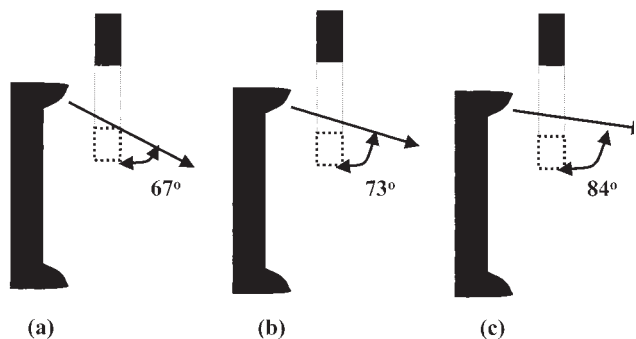


Figure 3: Jet angle relative to the ultrasound transducer measurement axis for experiments involving: a) the St. Jude Medical valve; b) the CarboMedics Model 700 valve; and c) the Sorin Bicarbon valve.

The power spectrum of the fluctuating velocity component was examined at each measurement location to check for the presence of periodic flow structures. As no peaks were apparent in these spectra, periodic flow structures did not contribute to error in these measurements. Subsequently, 95% confidence intervals for the turbulent normal stress calculations were created from an estimator variance of a second-order moment, assuming a normal distribution of velocity measurements within each combination of phase window and measurement location (23).

After correction for Doppler ambiguity and velocity gradient effects (19), maximum turbulent shear stresses were estimated from the measured turbulent normal stresses. The estimation technique was analytical, and applied the turbulent kinetic energy equation and a principal stress analysis to the flow geometry of an axisymmetric free jet. Details of the justification for this assumption, and the errors it can introduce into the calculation of turbulent shear stress (τ), have been described previously (19):

$$\tau_{\text{max}} = \frac{\sigma_x}{4 \left(\cos^2\theta_x + \frac{1}{2}\cos^2\theta_y + \frac{1}{2}\cos^2\theta_z \right)} \quad (4)$$

Results

Effects of driving pressure

Leakage flow across a mechanical prosthesis is partially governed by the pressure difference across the valve. The pressure difference across a mitral valve during the leakage phase is roughly equivalent to the left ventricular pressure. As the atrial pressure data of several experiments were deemed inaccurate due to a faulty pressure transducer, the left ventricular pressure alone was used to demonstrate the effects of pressure difference on leakage flow variables.

Figure 5(a) and (b) shows plots of the largest magnitudes of peak velocity and maximum turbulent shear stress from maximum velocity measurements for each jet studied as a function of the peak left ventricular pressure during the time that these particular measurements were acquired. The largest magnitudes of peak velocity and turbulent shear stress estimated from these experiments were 5.45 m/s and 92 N/m^2 , respectively. Though the data had considerable spread, there was a trend towards an increased turbulent shear stress with increased left ventricular pressure.

For this reason - and because there was a large variation in left ventricular pressure conditions between experiments - each experiment was placed into one of three discrete groups for analysis, based on the ranges of magnitude in left ventricular pressure observed during the experiments. An average of peak left ven-

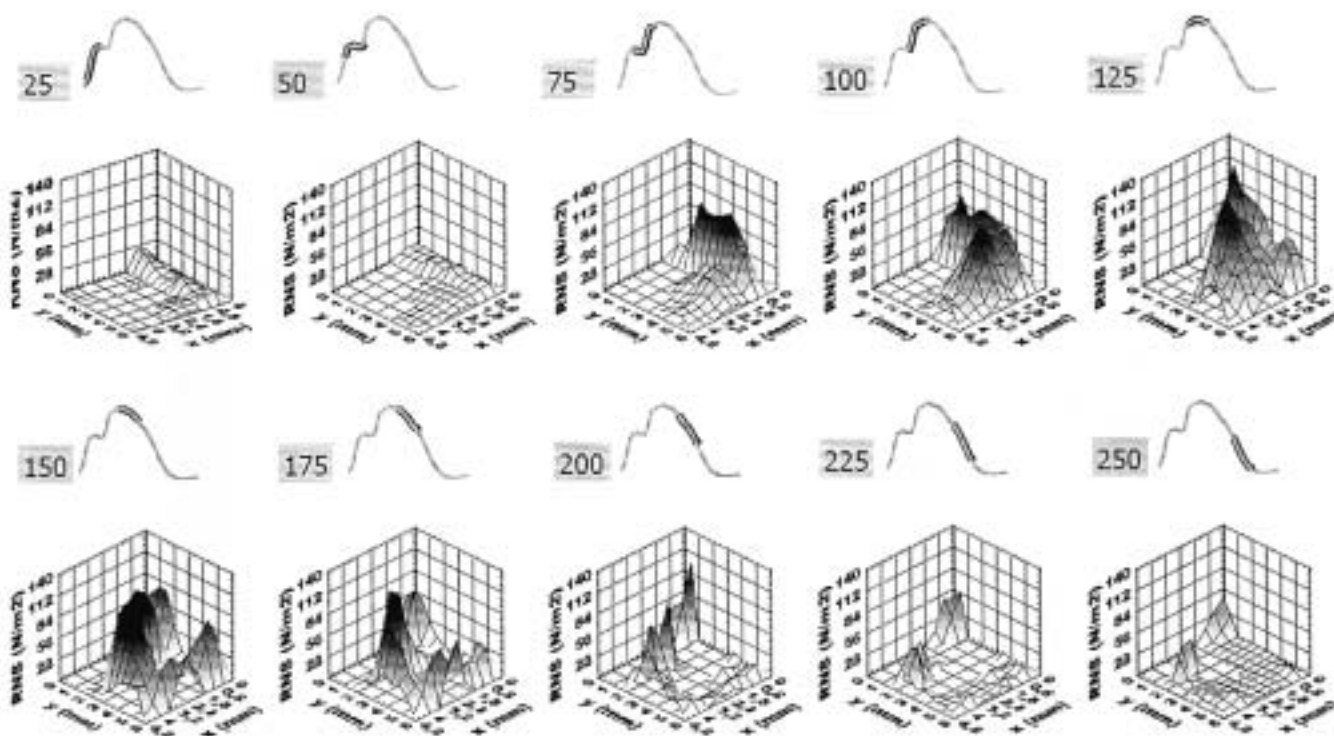


Figure 4: Example of temporal series of three-dimensional surface plots used to analyze data. In this figure, data from an MP valve was analyzed over a longer phase window than reported in the study in order to show the development of turbulence within the leakage over time in a small area. The three-dimensional plots in this figure show Reynolds normal stress (z-axis) as a function of position within the measurement area (x, y axes). The number above these plots represents the time after the start of systole during which the phase window begins. The curve above the three-dimensional plots represents the left ventricular pressure, and the darkened portion represents the temporal position of the phase window.

tricular pressure magnitudes was used to define these groups, where this average was equal to the sum of the minimum and maximum peak left ventricular pressure magnitudes (listed in Table I) divided by two. Experiments with an average peak left ventricular pressure magnitude <85 mmHg were considered in the low driving pressure group. The group of medium driving pressure consisted of experiments with average peak left ventricular pressure magnitudes between 85 and 130 mmHg, while the group of high driving pressure conditions experiments had average peak left ventricular pressure magnitudes >130 mmHg (Tables II-IV). Some results are not presented for the MP valve because the lack of knowledge of the MP jet angles relative to the housing prevented estimation of peak velocities and turbulent shear stresses. The average of the estimated peak velocities within the jets studied were 1.62, 2.58, and 4.51 m/s under low, medium, and high driving pressure conditions, respectively. The average of the estimated maximum turbulent shear stresses calculated from maximum velocity measure-

ments within the jets were 5, 14, and 58 N/m² under low, medium, and high driving pressure conditions, respectively.

Comparison of valve designs

At low driving pressure conditions, the maximum velocity measured within the leakage jets of the HL valve (0.67 m/s) was only slightly higher than that measured within the leakage of the SJ valve (0.62 m/s). Turbulent normal stresses calculated from mean velocity measurements within the HL jets were over double those of the SJ valve, but the largest turbulent normal stresses calculated from maximum velocity measurements were very similar between the two valves (12 and 11 N/m², respectively). Velocity and turbulent normal stress measurements calculated from maximum velocity measurements were considerably larger in the leakage of the MP valve than either the SJ or the HL valves at low driving pressure conditions. The largest turbulent normal stresses calculated from maximum velocity measurements within the leakage of the

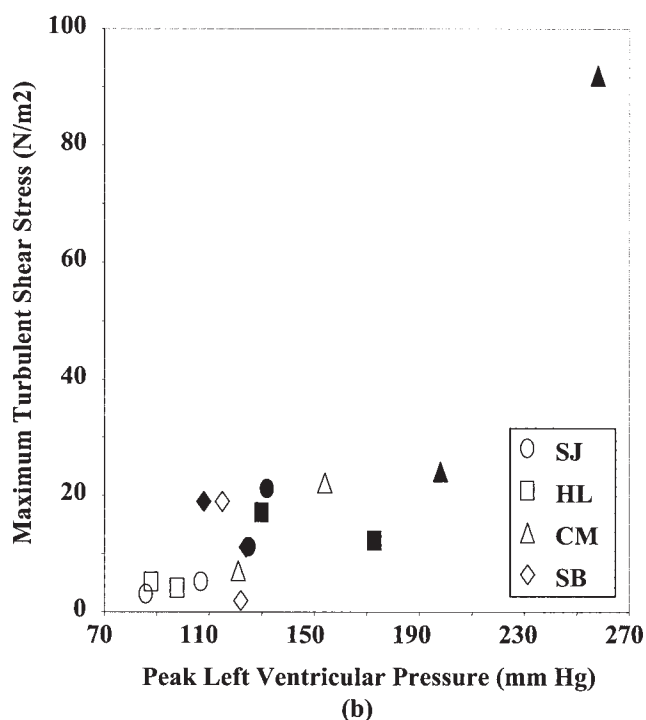
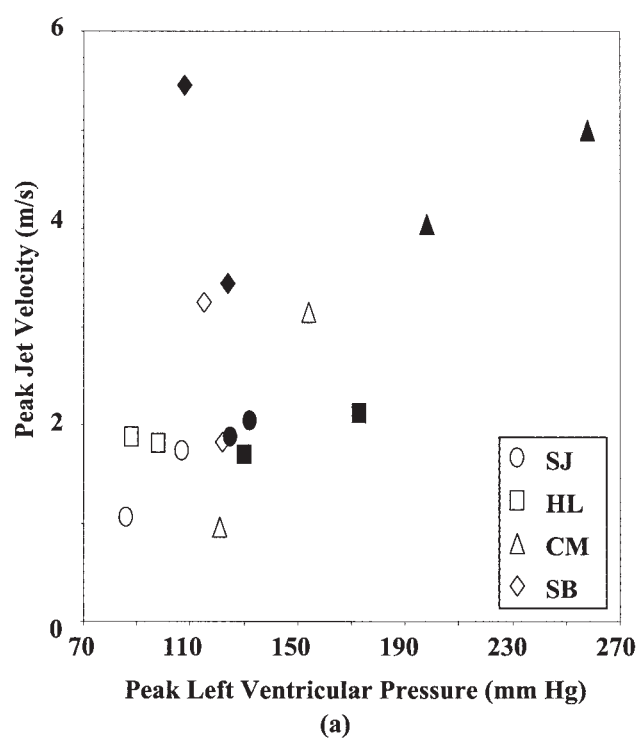


Figure 5: Peak left ventricular pressure versus estimations of (a) peak jet velocity and (b) maximum jet turbulent shear stress calculated from $u_{ij(max)}$. No data were available for the MP valve. Open symbols signify experiments performed in a resting state; filled symbols represent experiments performed in an exercise state.

MP valve (57 N/m^2) were over five-fold greater than those observed in the leakage jets of either the SJ or HL valves.

At medium driving pressure conditions, the largest leakage velocities in the direction of the transducer were measured in the jets of the HL valve (0.77 m/s), while the lowest velocities were in general measured in the jets of the SB valve. When these measurements were corrected by the predicted jet angle relative to the transducer direction, however, an unexpectedly high velocity was calculated for one of the jets of the SB valve (5.45 m/s). The SJ and HL valves had relatively small estimated peak velocities (2.04 and 2.12 m/s , respectively) in comparison to the CM and SB valves (3.15 and 5.45 m/s , respectively). The largest turbulent normal stresses calculated from maximum velocity measurements of the SJ, CM, SB, and HL valves were 47 , 47 , 38 and 38 N/m^2 , respectively. Estimated values of maximum turbulent shear stress from maximum velocity measurements were similar for all valves studied under these driving pressure conditions, falling within a range between 17 and 22 N/m^2 . The largest turbulent normal stresses calculated from mean velocity measurements were comparable for all valves except for the SJ valve, the leakage of which created stress magnitudes only up to 3 N/m^2 .

Leakage jet velocities measured along the transducer axis were similar (1.33 and 1.46 m/s) for the MP and CM valves under high driving pressure conditions. One of the pivots of the CM valve created turbulent normal stresses that were exceptionally high (36 and 199 N/m^2 , respectively, when calculated from mean and maximum velocity measurements) in comparison with others found in this series of experiments. The incoming forward flow surrounding this jet had a flow opposing the jet in the transducer direction with a maximum velocity of around 1 m/s . Such high incoming forward-flow velocities were not observed in any other experiments, and were observed on only one pivot of this valve. Leakage across the remaining pivot created turbulent stresses comparable to those observed in the MP valve leakage.

Discussion

Technique comparison with laser Doppler velocimetry

Before initiating a thorough analysis of the results of this investigation, it was important to realize some of its advantages, limitations, and differences from previous studies. Most previous studies of turbulence in the leakage jets of mechanical prostheses have been performed using laser Doppler velocimetry. A laser Doppler velocimeter records the velocity of each of a

Table II: 95% confidence intervals of the largest velocities and turbulent normal stresses measured within leakage jets of the low driving pressure group.

Jet	$(u_{00})_x$ (m/s)	u_{peak} (m/s)	σ_x (N/m ²)		τ_{max} (N/m ²)	
			$U_{ij(mean)}$	$U_{ij(max)}$	$U_{ij(mean)}$	$U_{ij(max)}$
SJ R1	0.62 ± 0.01	1.73	2 ± 0	11 ± 1	1	5
SJ R2	0.38 ± 0.02	1.06	2 ± 0	7 ± 1	1	3
HL R1	0.65 ± 0.01	1.81	5 ± 0	10 ± 1	2	4
HL R2	0.67 ± 0.02	1.87	6 ± 0	12 ± 1	3	5
MP R1	1.01 ± 0.03		5 ± 0	57 ± 5		
MP R2	0.98 ± 0.04		5 ± 0	47 ± 4		

Peak axial velocities and maximum turbulent shear stresses of the jets are also estimated within this table. Turbulent normal and shear stresses are reported both from mean and maximum velocity measurements. For details of jets, see Table I (footnote).

number of individual particles crossing its sample volume. After these velocities are recorded, they are averaged, and turbulent stresses are usually calculated from some form of the variation in velocity measurements. The technique in the present study - PDU - uses two different approaches. The ultrasound transducer transmits a burst of sound that is reflected from a large number of blood cells crossing its sample volume. Either the average or the maximal velocities of these blood cells are recorded from the reflected sound. Turbulent stresses are calculated from the variation of several of these averages or maxima.

The laser Doppler velocimeter measures the velocity of particles crossing a sample volume with dimensions on the order of 0.1 mm. Although this volume is small, it is finite in comparison with the diameter of a leakage jet created by a mechanical prosthesis, estimated by several studies to be on the order of 0.5 mm. Because of this, there is expected to be a considerable velocity gradient across the sample volume. This means that particles entering one side of a sample volume may be moving faster than particles entering the other. If each individual velocity measurement is averaged, this will result in a variation in velocity, even though there may be no turbulence. Most previous laser Doppler velocimetry studies are expected to overestimate calculations of turbulent shear stress and underestimate peak jet velocity as a result of the velocity gradient across the sample volume (24). Although the sample volume of the PDU is considerably larger than that of the laser Doppler velocimeter, velocity gradient contamination of the calculations of turbulent stresses in PDU are considerably reduced by using the average or maximum velocities of a large number of particles within the sample volume rather than individual

Table III: 95% confidence intervals of the largest velocities and turbulent normal stresses measured within leakage jets of the medium driving pressure group.

Jet	$(u_{00})_x$ (m/s)	u_{peak} (m/s)	σ_x (N/m ²)		τ_{max} (N/m ²)	
			$U_{ij(mean)}$	$U_{ij(max)}$	$U_{ij(mean)}$	$U_{ij(max)}$
SJ E1	0.73 ± 0.03	2.04	2 ± 0	47 ± 4	1	21
SJ E2	0.67 ± 0.02	1.87	3 ± 0	25 ± 2	1	11
CM R1	0.28 ± 0.02	0.96	12 ± 1	15 ± 1	6	7
CM R2	0.92 ± 0.02	3.15	7 ± 1	47 ± 4	3	22
SB R1	0.34 ± 0.02	3.25	9 ± 1	37 ± 3	5	19
SB R2	0.19 ± 0.01	1.82	2 ± 0	4 ± 0	1	2
SB E1	0.36 ± 0.01	3.44	6 ± 0	21 ± 2	3	11
SB E2	0.57 ± 0.02	5.45	5 ± 0	38 ± 3	3	19
HL E1	0.63 ± 0.02	1.70	4 ± 0	38 ± 3	2	17
HL E2	0.77 ± 0.03	2.12	11 ± 1	27 ± 2	5	12

Peak axial velocities and maximum turbulent shear stresses of the jets are also estimated within this table. Turbulent normal and shear stresses are reported both from mean and maximum velocity measurements. For details of jets, see Table I (footnote).

velocity measurements. This contamination amounted to no more than 2 N/m² in the present study (19), and was subtracted from calculations of the turbulent shear stresses before they were reported in Tables II-IV.

The laser Doppler velocimeter measures velocities over a sample volume close to an order of magnitude smaller than the PDU method used in the present study. For this reason, laser Doppler velocimetry has a much better spatial resolution than PDU. Since the sample volume of the ultrasound transducer used in the present studies had dimensions on the order of 1 mm, this transducer could not accurately measure jet width or shape. For this reason, jet width and shape were not reported.

The small size of the ultrasound sample volume relative to the leakage jet width also meant that the ultrasound technique of using several mean velocity measurements to calculate turbulent stress introduced error into the calculations. This error was associated with the fact that a considerable portion of the sample volume was located outside the turbulent portion of the jet, and its magnitude was dependent on the portion of the jet within the sample volume. Turbulent fluctuations detected by the transducer would therefore be dampened by averaging with velocity measurements obtained within the portion of the sample volume outside the jet, and the turbulent stress calculated by mean velocity measurements would be lower than the turbulent stress within the jet. Hence, the use of mean velocity measurements from the ultrasound transducer in turbulent stress calculations would be expected to underestimate turbulent stress magni-

Table IV: 95% confidence intervals of the largest velocities and turbulent normal stresses measured within leakage jets of the high driving pressure group.

Jet	$(u_{00})_x$ (m/s)	u_{peak} (m/s)	σ_x (N/m ²)		τ_{max} (N/m ²)	
			$U_{ij(mean)}$	$U_{ij(max)}$	$U_{ij(mean)}$	$U_{ij(max)}$
CM E1	1.18 ± 0.03	4.04	9 ± 1	53 ± 4	4	24
CM E2	1.46 ± 0.04	4.99	36 ± 3	199 ± 16	17	92
MP E1	1.33 ± 0.03		19 ± 2	61 ± 5		
MP E2	1.01 ± 0.03		10 ± 1	39 ± 3		

Peak axial velocities and maximum turbulent shear stresses of the jets are also estimated within this table. Turbulent normal and shear stresses are reported both from mean and maximum velocity measurements. For details of jets, see Table I (footnote).

tudes.

In contrast, the use of maximum velocity measurement within the sample volume to calculate turbulent stress is expected to overestimate turbulent stress magnitudes. Because the maximum velocity function measures the largest velocities within the sample volume at a given time, it can measure the movement of the largest turbulent eddies within a flow. As all turbulent energy originates in these larger eddies, the maximum velocity function can be used to measure turbulent stress. The potential problem with the use of this function is that the maximum velocity is measured independently of whether it moves toward or away from the transducer. Because of this, abrupt changes in velocity measurement could be caused by changes in the direction of maximum velocity observed by the transducer, which may not necessarily be due to turbulent eddies. In the present study, turbulent stresses were calculated from both mean and maximum velocity measurements to represent a range within which the actual value of turbulent stress should lie.

Angle correction

Another limitation of the PDU technique used in this study was that it was only able to measure velocity in one direction. For this reason it was necessary to use angle estimates from previous in-vitro studies (11,14) and an analytical technique to determine peak velocity and maximum turbulent shear stress. There may have been differences between the angles of the leakage jets estimated in the previous studies and those found in the present investigation, due to atrial inflow and differences in chamber geometry between in-vivo and in-vitro experiments, among other things. Angle-corrected velocity measurements have been found to

overestimate the peak velocity magnitude, due to the presence of out-of-plane velocity components within the sample volume (25). This overestimation would be expected to increase with the magnitude of the angle correction. An upper limit on leakage jet velocity can be obtained from Bernoulli's equation, which relates the pressure difference across a valve to the peak jet velocity if no viscous resistance were present. Under medium driving pressure conditions, Bernoulli's equation sets an upper limit of approximately 5.6 m/s on the peak velocity. As an appreciable amount of momentum is expected to be lost from viscous resistance, the validity of the peak jet velocity estimated for the SB valve (5.5 m/s) was very questionable. The ultrasound technique used in the present studies may, therefore, not be well suited for the calculation of peak jet velocities. The overestimation resulting from angle estimation and correction is not expected to greatly affect the velocity variation from which turbulent shear stresses are calculated.

Blood rheology

Blood is generally simulated in vitro with a Newtonian fluid - a fluid that has a linear relationship between velocity gradient and viscous shear stress. At shear rates above 500 s⁻¹, attractive forces between blood cells play only a small role in blood behavior, and mean velocity profiles can be simulated with a Newtonian analog (18). This is expected to occur along the edges of the leakage jets of heart valve prostheses, where velocity gradients can exceed 4,000 s⁻¹ (11). Because of this, peak leakage jet velocities measured using blood would be similar to those measured using Newtonian blood analogs under similar conditions.

Turbulent stresses, however, would be expected to be smaller in blood than in Newtonian analogs under similar conditions. This is partially due to the aforementioned attractive forces between blood cells, and partially due to the elastic nature of erythrocytes. The erythrocyte is an extremely flexible structure, capable of undergoing large membrane deformations and returning unscathed to its original shape (26). In addition, a velocity gradient applied to the surface of the erythrocyte would merely cause its membrane to rotate around its fluid contents. The attractive forces between blood cells and the viscoelastic nature of erythrocytes enable the blood to dissipate turbulent energy without damage. Flows with solutions of long-chain polymers at low concentrations have been found to have decreased turbulence in comparison with Newtonian fluids (18). Blood is expected to behave in a similar fashion.

Atrial chamber geometry

The geometry of the atrial chamber of the heart was

different from that of most previous in-vitro models in two notable aspects. The first is that the atrium was quite small in size, and leakage jets from the mitral valve impinged quickly on the atrial wall. In some experiments of the present investigation, measurements were attempted at an axial distance of 5 mm from the valve housing, and could not be collected because the sample volume of the transducer was located within the atrial wall. This short distance impingement would be expected to slightly reduce the peak velocity of the leakage jets, and it was unclear how this would affect turbulence within the jets. The second notable aspect was that forward flow entered the atrium in a direction nearly parallel to the plane of the valve housing, and the leakage jets of a mechanical prosthesis contacted the forward flow almost immediately after exiting the leakage gaps. Forward flow would affect both velocity and turbulent stress within the leakage jets. It could either increase or decrease the peak jet velocity, depending on the angle of the forward flow relative to the jet. Contact between the forward flow and leakage flow mixes two flows of different velocity and direction, resulting in the creation of turbulent stresses. Forward and leakage flows that oppose each other greatly in direction would be expected to generate large turbulent stresses.

Effects of exercise

Exercise can be expected to increase both heart rate and the driving pressure for leakage flow. While clear correlations between heart rate and leakage jet velocity could not be established, there was shown to be a correlation between left ventricular pressure and turbulent shear stress estimated from maximum velocity measurements (Fig. 5). Turbulent shear stress magnitudes would therefore be expected to increase significantly with exercise. The poor correlation between left ventricular pressure and leakage jet velocity relative to the correlation between left ventricular pressure and turbulent shear stress further suggests that overestimations due to angle correction may be responsible for inaccuracies in peak velocity estimation.

Comparison of valve designs

While velocities and turbulent shear stresses of the leakage jets are influenced by left ventricular pressure, these quantities are also influenced by other variables. One of these variables is valve design (Table II). The leakage jets of the MP valve had significantly higher peak velocities and turbulent normal stresses in the transducer direction than either the SJ or HL valve. Another of the variables to affect leakage jet velocity and turbulent shear stress was the leakage gap width. No significant turbulence could be detected in experiments with the LL valve, but turbulence shear stresses

were created by leakage from both the SJ and the HL valves.

The high turbulent normal stress found in the leakage of the MP valve relative to that found in the leakage of the SJ or the HL valves under low driving pressure conditions was expected. Flow over geometries with sharp corners, such as the cylindrical projection of the MP leaflet hinge, start to become disturbed at much lower Reynolds numbers than flow over geometries with smooth contours, such as the SJ hinge design. Since the Reynolds number of leakage flow rises with left ventricular pressure, the MP valve would become considerably turbulent at lower values of left ventricular pressure than the SJ valve. The MP valve has been shown previously to create more flow disturbance than the SJ hinge design, both within the pivot and in the exiting leakage flow in vitro (10,17,27).

The leakage jets of the SJ and HL valves were very similar, both in peak velocity and turbulent normal stress calculated from maximum velocity measurements. This could mean that the HL valve was just outside of leakage tolerances for the SJ design, and that the SJ valve studied was close to the upper leakage tolerance for this design.

Under medium driving pressure conditions, leakage of the SJ, CM, SB, and HL valves had similar magnitudes of turbulent shear stress, when calculated from maximum velocity measurements. When calculated from mean velocity measurements however, turbulent stresses within the leakage of the SJ valve were only slightly lower than those of the CM, SB, and HL valves. A previous laser Doppler velocimetry study conducted by Steegers et al. at medium driving pressure conditions supported this finding (11). In these studies, turbulent shear stresses were calculated analytically from SJ, CM, and SB leakage jet velocity gradients. It should be pointed out, however, that leakage jet turbulence could vary considerably from valve to valve due to the manufacturing tolerances of a given valve design.

The largest turbulent shear stresses magnitude estimated in these studies (92 N/m^2) was within only one jet of the CM valve under high driving pressure conditions. An examination of the velocity traces of the surrounding measurements indicated that this leakage jet was present in an area incoming forward flow with an average velocity of 1 m/s in the opposing direction. The strongly opposed momenta of the leakage jet and this forward flow likely created this exceptionally large stress. The remaining jet studied created turbulent shear stress magnitudes similar to those found in the MP valve under similar conditions.

Comparison with previous measurements

Most previous in-vitro studies of bileaflet valve leakage have been performed using laser Doppler

velocimetry under medium driving pressure conditions. Ellis et al. found a peak velocity of 0.8 m/s and maximum turbulent shear stresses of 80 N/m² at 1 mm proximal to one of the pivots of a SJ Standard size 27 mitral valve (10). Steegers et al. (11) performed a similar study on all four pivots of SJ, CM, and SB mitral valves, and found peak velocities of 1.0, 1.7, and 0.7 m/s and maximum turbulent stresses of 50, 80, and 60 N/m², respectively, within the leakage 1 mm proximal to these valves using laser Doppler velocimetry. Using PDU with very small angle correction, Steegers et al. also estimated peak velocities of 1.3, 0.9, and 0.8 m/s from the SJ, CM, and SB valves. Meyer et al. reported peak velocities of 0.7 and 2.3 m/s and maximum turbulent shear stresses of 45 and 360 N/m² from the leakage of SJ and CM mitral valves (13). Most recently, Travis et al. reported a peak velocity of 0.6 m/s and maximum turbulent shear stress of 27 N/m² from a SJ Regent size 17 aortic valve (14). Thus, under medium driving pressure conditions, in-vitro studies have reported peak jet velocities between 0.6 and 1.0 m/s for the SJ valve, between 1.7 and 2.3 m/s for the CM valve, and of 0.7 m/s for the SB valve. The largest maximum turbulent shear stresses have been reported to be between 27 and 80 N/m² for the SJ valve, between 80 and 360 N/m² for the CM valve, and 60 N/m² for the SB valve.

In the present study, peak velocities of 2.0, 3.2, and 5.5 m/s were estimated within the leakage of the SJ, CM, and SB valves respectively under medium driving pressure conditions. The differences between these and previous measurements may have been due to jet impingement on the atrial wall, differences in measurement techniques, or differences in incoming forward flow. Jet impingement on the atrial wall would be expected to lower velocities found in the present study relative to those of previous in-vitro studies. Instead, the peak velocities reported by the present studies were larger than those reported in previous investigations. Laser Doppler velocimetry is expected to underestimate jet peak velocity due to velocity gradients across the sample volume. However, the study of Steegers et al. showed that PDU using small correction angles agreed well with laser Doppler velocimetry measurements. Thus, laser Doppler velocimetry would be well suited to the measurement of peak velocity within leakage jets, and differences between these and previous measurements would most likely be due either to overestimation of jet peak velocity by PDU due to the measurement of out of plane velocity, or from differences in incoming forward flow.

Maximum turbulent shear stresses calculated from mean velocity measurements in the present study (1, 6, and 5 N/m², for the SJ, CM, and SB valves, respectively) were over an order of magnitude lower than those

reported in previous in-vitro studies. Turbulent shear stresses calculated from maximum velocity measurements (21, 22, and 19 N/m² for the SJ, CM, and SB valves) were also considerably lower than the range of those found in vitro. The study of Steegers et al. (11) used a large, open chamber, in which forward-flow contact with the leakage jets would be expected to be negligible. This should decrease the calculated turbulent shear stresses of their results relative to those of the present study, but this did not happen. Therefore, differences between the present findings and previous in-vitro results could result from differences in measurement techniques, or differences in fluid rheology.

Potential for blood damage

The results of the present study suggested that the blood damage potential of leakage flow could be considerably less than was previously thought. Almost all turbulent shear stresses estimated from the results of these experiments were well below blood damage thresholds reported for hemolysis or platelet disruption on a time scale comparable to 1 ms (4,28). The sole exception was the leakage flow measured proximal to the CM valve under high driving pressure conditions, which reached a turbulent shear stress of 92 N/m².

Leakage flow turbulence likely plays only a minor role in the total blood damage caused by blood flow around bileaflet prostheses, even if the maximum turbulent shear stresses created by the leakage of valves are as high as those reported in vitro. This can be seen by comparing blood exposure to leakage turbulence and forward-flow turbulence. Within a given heartbeat, the volume of blood exposed to forward flow is 30 to 40 times greater than the volume of blood exposed to leakage flow. Turbulent shear stresses measured in the forward flow of bileaflet prostheses (29-33) are the same as (or an order of magnitude greater than) those measured in leakage flow. In addition, the exposure time of cells to turbulent stresses during forward flow is an order of magnitude greater than the corresponding exposure time during leakage flow. The small length scales of the turbulent eddies which occur during leakage flow are sometimes stated as a reason that leakage flow turbulence is so damaging. However, the turbulent portion of forward flow in the jets immediately distal to the valve is composed of mixing layers approximately 1-2 mm in thickness. Within these mixing layers, turbulent eddies have length scales comparable to those expected during leakage flow. Because forward-flow turbulence affects a greater volume of blood than leakage-flow turbulence, creates stresses of magnitude equal or greater than those created by leakage flow turbulence, acts on cells for a longer time than leakage flow turbulence, and has small eddies of comparable size to leakage

flow turbulence, forward-flow turbulence is more likely to damage blood cells than leakage-flow turbulence.

It is important to distinguish the previous statement from the statement that forward flow is more likely to damage blood cells than leakage flow. Turbulence is one phenomenon that could result in blood damage, but others exist. Mechanical valves which create either high viscous stresses during leakage flow or cavitation could initiate blood damage irrespective of the amount of turbulence created by the valve. Preliminary studies have suggested that cavitation (34) and viscous stresses during leakage (35) may be very damaging to blood cells.

In conclusion, increases in left ventricular pressure, which could be brought about by exercise, cause increases in turbulent shear stresses within the leakage jets of bileaflet prostheses. Hinge design and leakage gap width can also affect the magnitudes of these stresses. Turbulent shear stresses that occur within the leakage jets may be smaller in magnitude than previously thought, and hold less potential for blood damage than forward-flow turbulence.

Acknowledgements

The authors thank Tanya Thomsen from the Institute of Experimental and Clinical Research and the perfusionists from the Department of Cardiothoracic and Vascular Surgery for their time and expertise in performing these experiments. They also thank St. Jude Medical, CarboMedics, Medtronic and Sorin Biomedica for their donation of the valves used in the study. The authors also wish to recognize the International Research Fellowship Program of the US National Science Foundation (Grant INT 0107348) for their generous financial support.

References

1. Bonow RO, Carabello B, de Leon AC, et al. ACC/AHA Guidelines for the Management of Patients With Valvular Heart Disease. Executive Summary. A report of the American College of Cardiology/American Heart Association Task Force on Practice Guidelines (Committee on Management of Patients With Valvular Heart Disease). *J Heart Valve Dis* 1998;7:672-707
2. Travis BR, Marzec UM, Leo HL, et al. Bileaflet aortic valve prosthesis pivot geometry influences platelet secretion and anionic phospholipid exposure. *Ann Biomed Eng* 2001;29:657-664
3. Meyer RS, Deutsch S, Maymir JC, Geselowitz DB, Tarbell JM. Three-component laser Doppler velocimetry measurements in the regurgitant flow region of a Björk-Shiley monostrut mitral valve. *Ann Biomed Eng* 1997;25:1081-1091
4. Lu PC, Lai HC, Liu JS. A reevaluation and discussion on the threshold limit for hemolysis in a turbulent shear flow. *J Biomech* 2001;34:1361-1364
5. Travis BR, Marzec UM, Ellis JT, et al. The sensitivity of indicators of thrombosis initiation to a bileaflet prosthesis leakage stimulus. *J Heart Valve Dis* 2001;10:228-238
6. Yoganathan AP. 2001. Personal Communication
7. Gross JM, Shu MC, Dai FF, Ellis J, Yoganathan AP. A microstructural flow analysis within a bileaflet mechanical heart valve hinge. *J Heart Valve Dis* 1996;5:581-590
8. Woo YR, Yoganathan AP. In vitro pulsatile flow velocity and shear stress measurements in the vicinity of mechanical mitral heart valve prostheses. *J Biomech* 1986;19:39-51
9. Baldwin JT, Tarbell JM, Deutsch S, Geselowitz DB. Mean velocities and Reynolds stresses within regurgitant jets produced by tilting disc valves. *Am Soc Artif Intern Organs Trans* 1991;37:M348-M349
10. Ellis JT, Healy TM, Fontaine AA, et al. An in-vitro investigation of the retrograde flow fields of two bileaflet mechanical heart valves. *J Heart Valve Dis* 1996;5:600-606
11. Steegers A, Paul R, Reul H, Rau G. Leakage flow at mechanical heart valve prostheses: Improved washout or increased blood damage? *J Heart Valve Dis* 1999;8:312-323
12. Maymir JC, Deutsch S, Meyer RS, Geselowitz DB, Tarbell JM. Effects of tilting disk heart valve gap width on regurgitant flow through an artificial heart mitral valve. *Artif Organs* 1997;21:1014-1025
13. Meyer RS, Deutsch S, Bachmann CB, Tarbell JM. Laser Doppler velocimetry and flow visualization studies in the regurgitant leakage flow region of three mechanical mitral valves. *Artif Organs* 2001;25:292-299
14. Travis BR, Leo HL, Shah PA, Frakes DH, Yoganathan AP. An analysis of turbulent shear stresses in leakage flow through a bileaflet mechanical prostheses. *J Biomech Eng* 2002;124:155-165
15. Ellis JT, Yoganathan AP. A comparison of the hinge and near-hinge flow fields of the St. Jude Medical hemodynamic plus and Regent bileaflet mechanical heart valves. *J Thorac Cardiovasc Surg* 2000;119:83-93
16. Saxena R, Lemmon J, Ellis J, Yoganathan A. An in vitro assessment by means of laser Doppler velocimetry of the Medtronic advantage bileaflet mechanical heart valve hinge flow. *J Thorac Cardiovasc Surg* 2003;126:90-98
17. Leo HL, He Z, Ellis JT, Yoganathan AP. Microflow fields in the hinge region of the CarboMedics bileaflet mechanical heart valve design. *J Thorac Cardiovasc Surg* 2002;124:561-574

18. Pohl M, Wendt MO, Werner S, Koch B, Lerche D. In vitro testing of artificial heart valves: Comparison between Newtonian and non-Newtonian fluids. *Artif Organs* 1996;20:37-46
19. Travis BR, Christensen TD, Smerup M, Olsen MS, Hasenkam JM, Nygaard H. An in vivo method for measuring turbulence in mechanical prosthesis leakage jets. *J Biomech Eng* 2004;126:26-35
20. Skoularigis J, Essop MR, Skudicky D, Middlemost SJ, Sareli P. Frequency and severity of intravascular hemolysis after left-sided cardiac valve replacement with Medtronic Hall and St. Jude Medical prostheses, and influence of prosthetic type, position, size and number. *Am J Cardiol* 1993;71:587-591
21. Ismeno G, Renzulli A, Carozza A, et al. Intravascular hemolysis after mitral and aortic valve replacement with different types of mechanical prostheses. *Int J Cardiol* 1999;69:179-183
22. Nygaard H, Hasenkam JM, Pedersen EM, Kim WY, Paulsen PK. A new perivascular multi-element pulsed Doppler ultrasound system for in vivo studies of velocity fields and turbulent stresses in large vessels. *Med Biol Eng Comput* 1994;32:55-62
23. Benedict LH, Gould RD. Towards better uncertainty estimates for turbulent statistics. *Exp Fluids* 1996;22:129-136
24. Petrie H, Samimy M, Addy A. Laser Doppler velocity bias in separated turbulent flows. *Exp Fluids* 1988;6:80-88
25. Yoganathan AP, Recusani F, Valdez-Cruz L, Sung HW, Sahn DJ. Oblique flow vectors from dispersing jets produce the velocity overestimation on angle corrected continuous wave Doppler studies: In vitro laser Doppler investigations. *Circulation* 1987;76(Suppl.IV):353-355
26. Evans EA, Hochmuth RM. Membrane viscoelasticity. *Biophys J* 1976;16:1-11
27. Zimmer R, Steegers A, Paul R, Affeld K, Reul H. Velocities, shear stresses and blood damage potential of the leakage jets of the Medtronic Parallel bileaflet valve. *Int J Artif Organs* 2000;23:41-48
28. Klaus S, Korfer S, Mottaghy K, Reul H, Glasmacher B. In vitro blood damage by high shear flow: Human versus porcine blood. *Int J Artif Organs* 2002;25:306-312
29. Barbaro V, Grigioni M, Daniele C, D'Avenio G, Boccanera G. 19 mm sized bileaflet valve prostheses flow field investigated by bidimensional laser Doppler velocimetry. *Int J Artif Organs* 1997;20:622-636
30. Fontaine A, Ellis J, Healy T, Hopmeyer J, Yoganathan A. Identification of peak stresses in cardiac prostheses: A comparison of two dimensional versus three dimensional principle stress analyses. *Am Soc Artif Intern Organs J* 1996;42:154-163
31. Giersiepen M, Wurztlinger L, Opitz R, Reul H. Estimation of shear stress-related blood damage in heart valve prostheses - in vitro comparison of 25 aortic valves. *Int J Artif Organs* 1990;13:300-306
32. Liu J, Lu P, Chu S. Turbulence characteristics downstream of bileaflet aortic valve prostheses. *J Biomech Eng* 2000;122:118-124
33. Tiederman W, Steinle M, Phillips W. Two-component laser velocimeter measurements downstream of heart valve prostheses in pulsatile flow. *J Biomech Eng* 1988;108:59-64
34. Garrison L, Lamson T, Deutsch S, Geselowitz D, Gaumond R, Tarbell J. An in-vitro investigation of prosthetic heart valve cavitation in blood. *J Heart Valve Dis* 1994;3(Suppl.1):S8-S24
35. Tillman W, Reul H, Herold M, Bruss K, Van Gilse J. In-vitro wall shear measurements at aortic valve prostheses. *J Biomech* 1984;17:263-279